Article

Synthesis and Characterization of Alternating Polymers Incorporating Boron-Chelated Heterochrysene Units

Hailei Zhang, Shuli Ma, Dongqin Li, Yonggang Wu and Xinwu Ba *

College of Chemistry and Environmental Science, Hebei University, Baoding, 071002, China;
E-Mails: haileipoly@126.com (H.Z.); m3538833@126.com (S.M.); ldq1039356629@163.com (D.L.);
wuyonggang@hbu.edu.cn (Y.W.)

* Author to whom correspondence should be addressed; E-Mail: Baxw@mail.hbu.edu.cn;
    Tel.: +86-312-5079317; Fax: +86-312-5079317.

Academic Editor: Alexander Böker

Abstract: The novel boron-chelated π-conjugated polymers named as **BF$_2$-poly** and **BPh$_2$-poly** were synthesized by a feasible condensation-chelation strategy. First, conjugated polymers bearing Boc group were prepared by using palladium-catalyzed Suzuki–Miyaura coupling reaction. Then, conjugated polymers (**poly-1**) were obtained with high efficiency by removing the Boc group from **Boc-poly**. Last, boron trifluoride diethyl etherate (BF$_3$·Et$_2$O) or triphenylboron (BPh$_3$) chelated with **poly-1** forming the target polymers. Furthermore, the boron-chelated polymers were characterized by UV−Vis absorption spectroscopy, photoluminescence spectroscopy, cyclic voltammetry and thermogravimetric analysis. As expected, fluorescences peaks at 520 nm and 592 nm were observed in diluted CH$_2$Cl$_2$. In addition, **BF$_2$-poly** and **BPh$_2$-poly** showed strong fluorescence at 545 nm and 601 nm in homogeneous solid state. The results coming from thermogravimetric analysis and cyclic voltammetry also revealed that the conjugated polymers have favorable electrochemical and thermostable properties.

Keywords: π-conjugation polymers; boron-chelated; heterochrysene; fluorescence properties

1. Introduction

In the past decades, π-conjugated derivatives have attracted significant interests in organic light-emitting diodes, field effect transistors, photovoltaic cell and fluorescent probes due to their unique characteristics such as high brightness, tunable emission, stability against photobleaching and high photon-emission rates [1–8]. In the early 1960s, Clar developed the first synthetic acene as a kind of π-conjugated derivative [9–11]. Since then, there has been continuing interest in the development of novel types of acenes in both academia and industry [12–17]. Among these π-conjugated derivatives, chrysene is a relatively special acene with a mismatch structure compared with tetracene, which captured some scholars' attention in recent years, especially after the introduction of boron into the skeleton.

π-conjugated boron complexes are gaining increasing attention because they can be utilized as catalyst, phototherapy drugs and luminescent device [18–21]. It is known that boron is strongly electrophilic by virtue of its tendency to fill the vacant orbital and complete the octet. Therefore, π-conjugated boron complexes possess more stable properties than metal-complexes [22,23]. In addition, the strongly electrophilic property may result in larger Stokes shifts, stronger bathochromic shifts and higher fluorescence quantum yields. Usually, $BF_3 \cdot Et_2O$ and BPh_3 were used as boron chelating agents to prepare π-conjugated boron complexes. In addition, BPh_2 complex possess a stronger bathochromic shift than BF_2 complex because of an enhanced conjugation degree as well as the biphenyl boron chelation. Since the stronger electron-withdrawing property, BF_2 complex often creates more efficient absorption and luminescence properties. In addition, boron will also bring novel function to π-conjugated polymers. Nagai *et al.* developed a condensation-chelation model method to prepare the first main-chain-type organoboron 1,3-diketonate polymers via Sonogashira–Hagihara coupling reaction and using BPh_3 or $(C_6F_5)BF \cdot OEt_2$ as chelating agents [24]. Jäkle *et al.* showed that novel well-defined organoboron quinolate polymers have succeeded in emission color-tuning of organoboron quinolate polymers from blue to red regions by treatment with substituted 8-hydroxyquinoline derivatives [25].

Recently, our group reported the boron-chelated *N,O*-bidentate chrysene analogues in Scheme 1 [26]. As obtained two novel boron-based chrysene analogues (Compound **1** and **2**) were synthesized by chelating with $BF_3 \cdot Et_2O$ or BPh_3, emitting strong green and yellow light in methylene chloride with high quantum yields. The objective of our study was to synthesize organoboron heterochrysene polymers by chelating reaction of heterochrysene based polyfluorene derivative as a polymeric ligand with $BF_3 \cdot Et_2O$ or BPh_3. Compound **4** was transformed into a di-brominated monomer followed by copolymerizing with di-borylated fluorene via the palladium-catalyzed Suzuki–Miyaura coupling reaction. All the boron-chelated polymers can be easily dissolved in common organic solvents such as dichloromethane and tetrahydrofuran (THF) to obtain good quality amorphous films. Focus has been drawn to the optical characteristics and electrochemical properties.
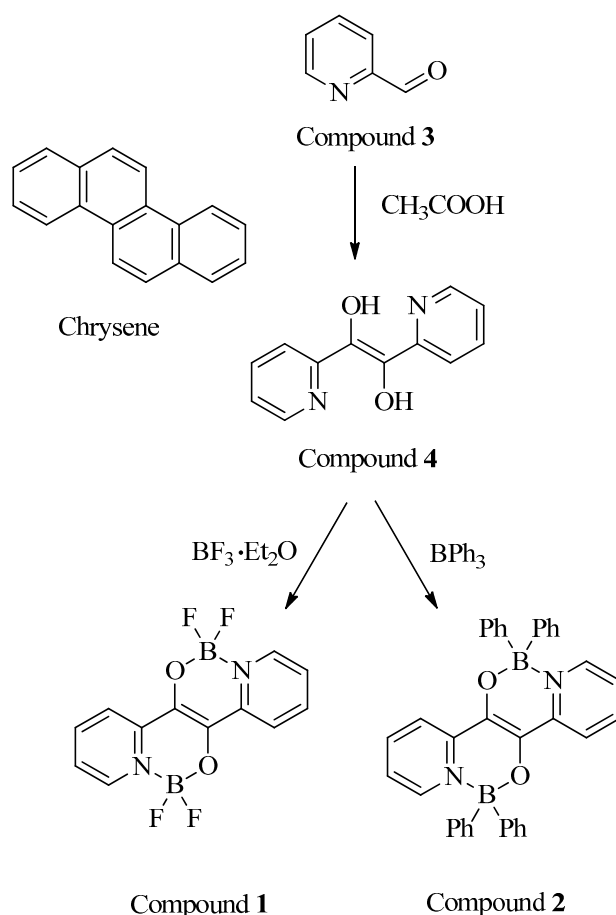
Scheme 1. The synthesis route of Compounds **1** and **2**.

2. Experimental Section

2.1. Materials and Methods

6-bromopyridine-2-carboxaldehyde (Compound **7**) was purchased from J&K Chemical Technology (Beijing, China) and used without further purification. Monomer **6** (2,7-bis(4,4,5,5-tetramethyl-1,3,2-dioxaborolan-2-yl)-9,9-dicetylfluorene) and the catalyst Pd(PPh$_3$)$_4$ were prepared according to the literature [27,28]. THF and CH$_2$Cl$_2$ used in reactions were dried and distilled from sodium and CaH$_2$. Distilled water was used throughout the study. High-purity argon was used for degassing procedures.

2.2. Synthesis of Monomer **5**

Thiamine (175 mg, 1.08 mmol) and tetrabutylammonium hexafluorophosphate (4 mg, 0.01 mmol) were dissolved in methanol-water (15 mL:3 mL) mixed solvent. Then sodium hydroxide aqueous solution (10%) was dropped into the above mixture to achieve a weakly alkaline solution (pH 9). After the addition of 6-bromopyridine-2-carboxaldehyde (Compound **7**, 200 mg, 1.08 mmol), the mixture was stirred and heated at 65 °C for 3 h. Then the reaction was quenched by addition of excess water to favor the precipitation of a yellow solid. The crude product was collected through centrifugation and washed thoroughly by methanol. The residue was chromatographically purified on silica gel eluting with petroleum ether/CH$_2$Cl$_2$ (1:1) to afford a yellow powder (50 mg). The obtained powder was directly

dissolved in anhydrous THF (4 mL) containing di-*tert*-butyl dicarbonate (292 mg, 1.34 mmol) and *N,N*-Dimethylaminopyridine (5 mg, 0.04 mmol). The reaction mixture was heated at 45 °C and stirred for 10 h. Excess methanol was added to quench the reaction to give a white precipitation. After centrifugation, the crude product was recrystallized from CH_2Cl_2/methanol to give a white needle of monomer **5** (55 mg, 0.096 mmol, 17.8%). ^1H NMR (600 MHz, $CDCl_3$, δ): 7.71 (d, J = 7.86 Hz, 2H; Ar–H), 7.53 (t, J = 15.72 Hz, 2H; Ar–H), 7.35 (d, J = 7.86 Hz, 2H; Ar–H), 1.43 (s, 18H; CH_3); ^{13}C NMR (150 MHz, $CDCl_3$, δ): 151.90, 150.20, 141.40, 140.03, 138.64, 127.90, 122.16, 84.49, 27.65; FT-IR (KBr): 3038, 2986, 2960, 2933, 2876, 1765, 1575, 1548, 1434, 1399, 1368, 1257, 1120, 1077, 980, 857, 799, 764, 671; Anal. Calcd for $C_{22}H_{24}Br_2N_2O_6$: C, 46.18; H, 4.23; N, 4.90. Found: C, 46.17; H, 3.94; N, 4.83.

2.3. Synthesis of **Boc-poly**

A mixture of monomer **5** (172 mg, 0.3 mmol), 2,7-bis(4,4,5,5-tetramethyl-1,3,2-dioxaborolan-2-yl)-9,9-dicetylfluorene (monomer **6**, 260 mg, 0.3 mmol) and $NaHCO_3$ (0.4 g) in THF–water (25 mL:4 mL) mixed solvent was carefully degassed. After the addition of $Pd(PPh_3)_4$ (17 mg, 0.015 mmol), the solution was fluxed for 120 h under stirring. Excess CH_2Cl_2 and water were added to quench the reaction and extract the product. The organic layer was separated and dried over Na_2SO_4. After removal of most of the solvent, the residue was precipitated in methanol to give **Boc-poly** as a brown solid (Yield = 63%). ^1H NMR (600 MHz, $CDCl_3$, δ): 7.45–8.20 (m, 12H), 1.63–2.27 (m, 4H), 1.23–1.35 (m, 12H), 0.27–1.23 (m, 68H); FT-IR (KBr): 3059, 2924, 2850, 1768, 1724, 1568, 1448, 1369, 1245, 1124, 983, 873, 804, 762.

2.4. Synthesis of **poly-1**

Piperidine (66 μL, 0.67 mmol) was dissolved in anhydrous CH_2Cl_2 (50 mL) containing **Boc-poly** (200 mg, 0.016 mmol). The mixture was then stirred at room temperature for 48 h. After centrifugation, the supernatant was concentrated in vacuum. The residue was precipitated in methanol to give **poly-1** as a brown solid (Yield = 83%). ^1H NMR (600 MHz, $CDCl_3$, δ): 7.37–8.44 (m, 12H), 0.19–2.27 (m, 73H); FT-IR (KBr): 3307, 3059, 2925, 2850, 1708, 1560, 1452, 1261, 1016, 808, 667.

2.5. Synthesis of **BF₂-poly**

A mixture of **poly-1** (50 mg, 0.005 mmol) and boron trifluoride–ethyl ether complex (1.0 mL, 46.5%) in anhydrous methylene chloride (5 mL) was stirred at room temperature for 6 h under argon atmosphere. The solution was then directly dropped into excess diethyl ether to favor a crude precipitate. After certification, the residue was then washed thoroughly by ether to give **BF₂-poly** as an orange solid (Yield = 86%). ^1H NMR (600 MHz, $CDCl_3$, δ): 7.24–9.00 (m, 12H), 0.20–2.37 (m, 80H); ^{13}C NMR (150 MHz, $CDCl_3$, δ) 155.84, 151.10, 150.77, 140.79, 136.96, 120.28, 119.16, 39.15, 30.90, 29.13, 28.68, 28.34, 22.70, 21.66, 13.09; FT-IR (KBr): 3080, 2919, 2848, 1618, 1564, 1483, 1323, 1246, 1147, 1109, 1047, 926, 858, 785.

2.6. Synthesis of *BPh₂-poly*

A mixture of **poly-1** (50 mg, 0.005 mmol) and BPh₃ in anhydrous THF (5 mL) was stirred at room temperature for 24 h under argon atmosphere. The solution was then directly dropped into excess *n*-pentane to favor a crude precipitate. The residue was then washed thoroughly by *n*-pentane to give **BPh₂-poly** as a red solid (Yield = 79%). ^{1}H NMR (600 MHz, CDCl₃, δ): 6.20–9.25 (m, 32H), 0.25–1.95 (m, 80H); ^{13}C NMR (150 MHz, CDCl₃, δ): 155.83, 151.04, 150.85, 136.93, 135.67, 134.64, 133.69, 132.23, 131.69, 130.04, 128.56, 127.73, 127.32, 126.98, 126.91, 126.35, 126.17, 124.55, 122.89, 120.31, 119.14, 118.40, 114.34, 54.03, 39.10, 38.48, 30.90, 29.13, 28.98, 28.68, 28.34, 28.24, 22.81, 22.71, 21.66, 13.08. FT-IR (KBr): 3062, 3008, 2919, 2850, 1608, 1562, 1475, 1304, 1219, 1149, 935, 783, 746, 706.

2.7. Characterizations

^{1}H (600 MHz) and ^{13}C (150 MHz) nuclear magnetic resonance (NMR) were performed on a Bruker AV600 spectrometer using tetramethylsilane as internal standard. Fourier transform infrared spectroscopy (FT-IR) of the samples was recorded using a Varian 640-IR instrument (Varian, Palo Alto, CA, USA). The electrochemical behaviors were investigated in the solid state by cyclic voltammetry (CV) in anhydrous acetonitrile solution at room temperature. A three-electrode electrochemical cell was used, which was comprised of a working electrode (glassy carbon electrode), a platinum mesh auxiliary electrode, and an Ag/AgNO₃ reference electrode. Furthermore, 0.1 M tetrabutylammonium hexafluorophosphate (TBAPF6) was used as a supporting electrolyte. The oxidation potentials were measured *versus* a standard ferrocene/ferrocenium redox system as the internal standard for estimating the highest occupied molecular orbital (HOMO) and lowest unoccupied molecular orbital (LUMO) of the boron-chelated polymers films. The scan rate was 50 mV·s^{-1}. Thermogravimetric analysis (TGA) was measured by TGA (Pyris-6, Perkin-Elmer, Waltham, MA, USA) operated under 20 mL/min nitrogen flow rate at the heating rate of 10 °C/min. UV–vis and fluorescence spectra were obtained through a UV2550 UV–Vis spectrophotometer (Shimazu, Japan) and an RF5301PC fluorescence spectrophotometer (Shimazu, Japan), respectively. Number-average molecular weight (M_n) and the molecular weight distribution (M_w/M_n) were measured via gel permeation chromatography (GPC) (Waters, Milford, MA, USA) with a system-equipped Waters HT4 and HT3 column-assembly and a Waters 2414 refractive index detector. The column was placed under 30 °C; the system was operated at a flow rate of 1.0 mL/min with THF as an eluent. Polystyrene was used as standards for the calibration. Film X-ray diffraction (XRD) patterns were performed at room temperature with a D8 ADVANCE X-ray power diffractometer system (Bruker, Faellanden, Switzerland). The patterns were recorded on a quartz plate at a tube voltage of 40 kV and a current of 40 mA over a 2θ range of 10°–90° using a step size of 0.01° at a scan speed of 1 s/step.

3. Results and Discussion

3.1. Synthetic Approach and Characterizations

As shown in Scheme 2, a symmetrical di-brominated monomer (**5**) was synthesized by a benzoin condensation of 6-bromopyridine-2-carboxaldehyde (**7**), where thiamine and tetrabutylammonium

hexafluorophosphate were used as catalysts. The product was directly treated with excess di-*tert*-butyl dicarbonate ester (Boc2O), aiming to eliminate the intermolecular cross-linking effect by hydrogen bonding between hydroxyl proton and oxygen atom in enol forms. The structure of 5 was confirmed by FT-IR (shown in Figure S1), elemental analysis and NMR (shown in Figures S2 and S3). Monomer **6** was synthesized following a procedure described elsewhere [27]. Monomers **5** and **6** were equimolarly mixed, where Pd(PPh3)4 was used as catalyst. Obtained **Boc-poly** was treated with piperidine under mild conditions. The reacting solution was centrifuged to remove some insolubles formed in deprotection reaction and the supernatant was concentrated and then precipitated into methanol to give **poly-1**. **Poly-1** was further reacted with excess BF3·Et2O or BPh3 in anhydrous CH2Cl2 or THF to give **BF2-poly** and **BPh2-poly**. All the polymers exhibited desirable solubility in THF, CH2Cl2 and chloroform.
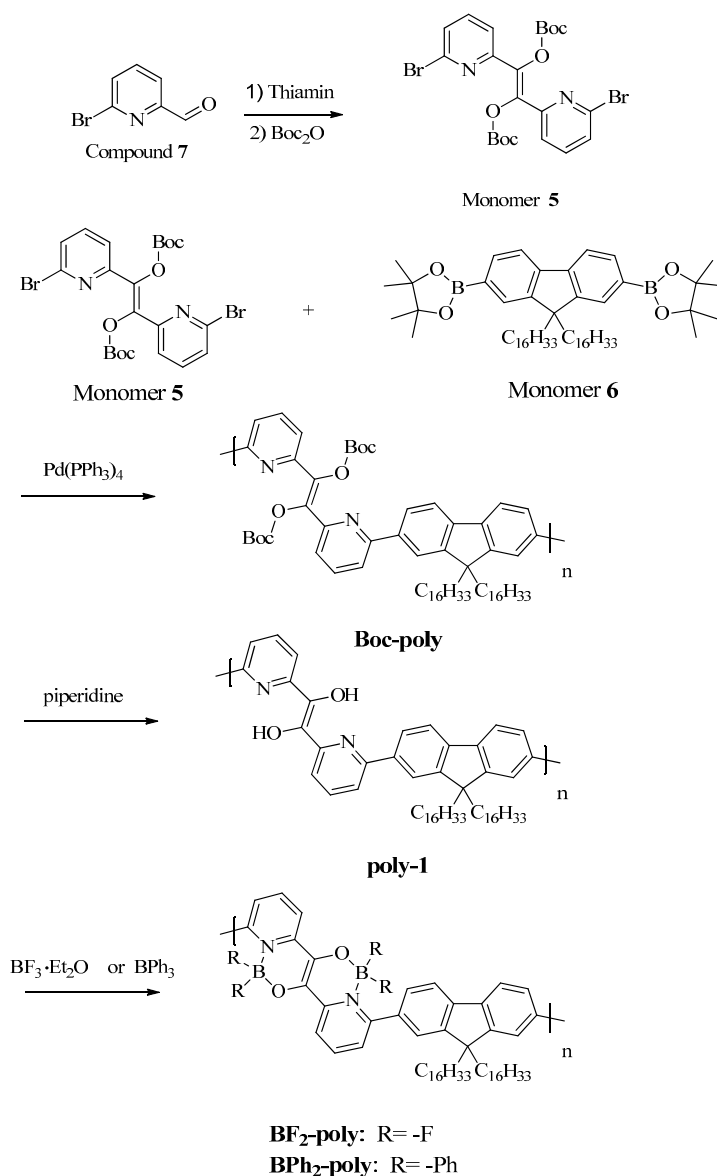

Scheme 2. The synthesis route of conjugated polymers.

The elution curves and GPC Data for obtained polymers were shown in Figure 1 and Table 1, respectively. The M_n and M_w/M_n of **Boc-poly** were determined as 1.41×10^4 Da and 3.17, respectively. **Poly-1** exhibited a lower molecular weight ($M_n = 1.03 \times 10^4$ Da) and a narrower distribution

(M_w/M_n = 1.93). After chelating reactions, the M_n of **BF$_2$-poly** and **BPh$_2$-poly** were 1.13 × 10^4 Da and 1.24 × 10^4 Da with polydispersity indexes being 1.86 and 2.12, respectively.

Table 1. Summary of gel permeation chromatography (GPC) data for obtained polymers.

| No.	M_n	M_w	M_w/M_n
Boc-poly	1.41 × 10^4 g/mol	4.47 × 10^4 g/mol	3.17
poly-1	1.03 × 10^4 g/mol	1.99 × 10^4 g/mol	1.93
BF$_2$-poly	1.13 × 10^4 g/mol	2.10 × 10^4 g/mol	1.86
BPh$_2$-poly	1.24 × 10^4 g/mol	2.63 × 10^4 g/mol	2.12
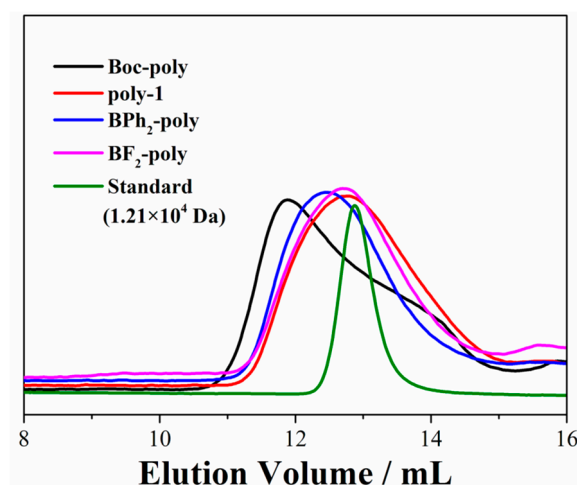
Figure 1. GPC elution curves.

The signals in the ^{1}H NMR spectra of the polymers can be classified into two groups (shown in Figures S4–S7): the signals that emerged at 7.3–8.3 ppm can be attributed to the aromatic protons; and the peaks ranging from 0.5 to 2.5 ppm can be assigned to the hydrogen atoms in alkyl groups. It is worth noting that the distinct signal at 1.29 ppm in the ^{1}H NMR spectrum of **Boc-poly** represents the hydrogen in Boc groups (shown in Figure S4). The disappearance of the peak at 1.29 ppm in the ^{1}H NMR spectrum of **poly-1** suggested that the deprotection reaction was completed (shown in Figure S5). The ^{1}H NMR spectrum of **BF$_2$-poly** showed a similar tendency to that of **poly1** (shown in Figure S6). However, compared to those of **poly-1** and **BF$_2$-poly**, the integral of the aromatic protons in **BPh$_2$-poly** increased more than double, which coincided with expected structures (shown in Figure S7). The ^{13}C NMR spectra of **BF$_2$-poly** and **BPh$_2$-poly** were illustrated in Figures S8 and S9, respectively.

The FT-IR spectra of the polymers were shown in Figure 2. **Boc-poly** displayed a characteristic absorption band around 1768 cm^{-1} in FT-IR spectrogram, which can be attributed to the C=O stretching in Boc groups. After deprotection, the disappearance of the C=O stretching in FT-IR spectrogram of **poly-1** also suggested that the deprotection reaction was completed. Meanwhile, FT-IR analysis showed that **poly-1** contained –OH group (3307 cm^{-1}), which can be assigned to the hydroxyl group coming from 2,2'-pyridoin-based ligand. The FT-IR spectra of **BF$_2$-poly** and **BPh$_2$-poly** showed the disappearance of –OH group, suggesting the chelating reactions were completed. The XRD patterns of **BF$_2$-poly** and **BPh$_2$-poly** are shown in Figure 3. The samples displayed no distinct peaks from 10° to 90°, suggesting the polymers existed in an amorphous form rather than crystals.

The thermal properties of monomer **5** and polymers were studied by thermogravimetric analysis (shown in Figure 4). The monomer showed a desirable thermostability with an onset temperature of weight loss (5%) at 375 °C. The onset temperatures of weight loss (5%) of **BF₂-poly** and **BPh₂-poly** were 288 °C and 248 °C, respectively, suggesting a higher thermal stability than **poly-1** (220 °C).
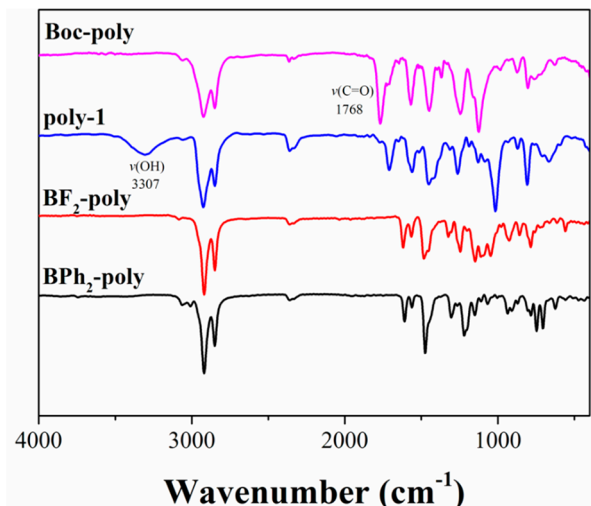
Figure 2. Fourier transform infrared spectroscopy (FT-IR) spectra of the obtained polymers.
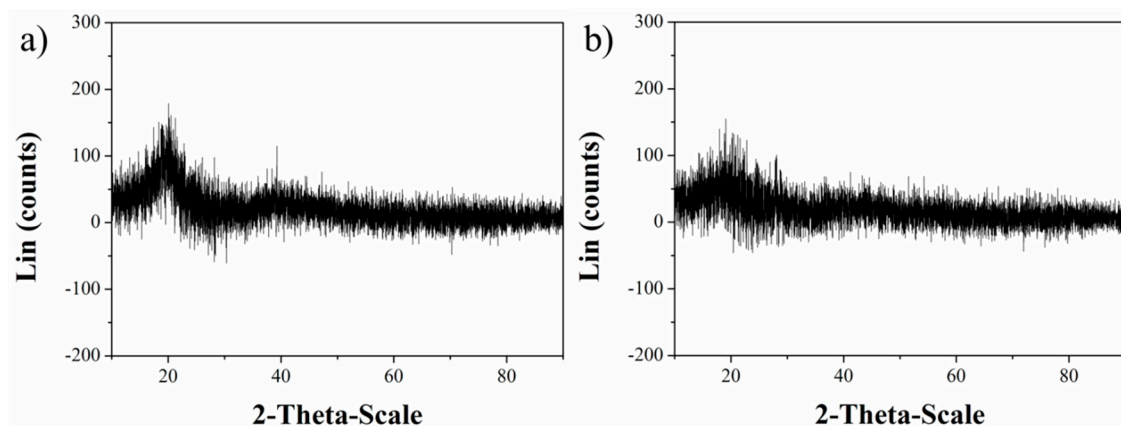
**Figure 3.** Film X-ray diffraction (XRD) patterns of **BF₂-poly** (**a**) and **BPh₂-poly** (**b**).
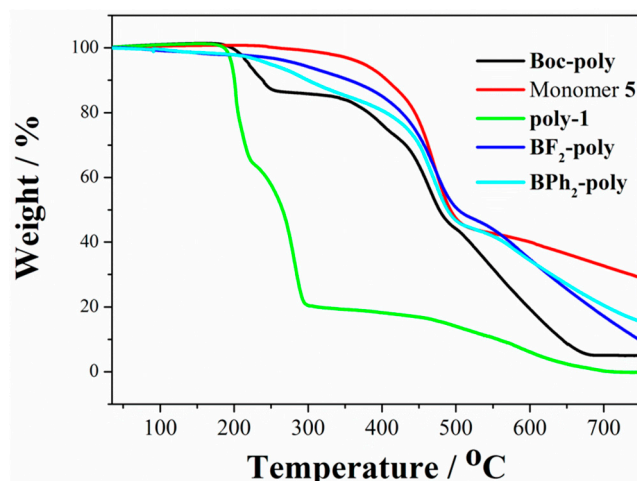
Figure 4. Thermogravimetric analysis (TGA) curves at a heating rate of 10 °C/min⁻¹.

3.2. UV–vis Absorption and Photoluminescence Studies

The UV–vis absorption spectra were measured in diluted CH_2Cl_2 solution, as shown in Figure 5a. The detail data were shown in Table 2. Boron-based heterochrysene derivatives (**1** and **2**) displayed maximum absorption peak at 410 and 468 nm. The wavelengths of maximum absorption of **BF₂-poly** (433 nm) and **BPh₂-poly** (481 nm) were high compared to those of **1** and **2**, because of the extended conjugation after polymerization. Otherwise, the relative electron-donating ability of the phenyl units can form an intramolecular charge-transfer system in D-p-A system, resulting in a significant difference between **BF₂-poly** and **BPh₂-poly** [26]. The biphenyl boron chelation in **BPh₂-poly** resulted in a stronger bathochromic-shift. Photoluminescence behaviors were also investigated in diluted CH_2Cl_2, as shown in Figure 6. **BF₂-poly** and **BPh₂-poly** displayed emission peaks at 520 nm and 592 nm, respectively. **BF₂-poly** and **BPh₂-poly** showed obvious bathochromic-shift compared to the corresponding compounds. The quantum yields (Φ_f) of **BF₂-poly** and **BPh₂-poly** were calculated as 0.23 and 0.11, respectively, where *N,N'*-di(2,6-diisopropylphenyl)-perylene-3,4,9,10-tetracarboxylic acid bisimide ($\Phi_f = 1.00$ in chloroform) was used as the reference standard [29]. It should be noted that boron-chelated polymers exhibited decreased fluorescence quantum compared to those of **1** and **2**, respectively. The decreased fluorescence quantum yields of boron-chelated polymers may be partly because of the unrestricted rotation around the C–C bond connecting chrysene unit to fluorene unit in noncoplanar conjugated polymers. Otherwise, 100% chelating ratios of **BF₂-poly** and **BPh₂-poly** were difficult to achieve. A small quantity of 2,2'-pyridoin groups may still exist in the boron-chelated polymers, which may also contribute to decreased fluorescence quantum yields.
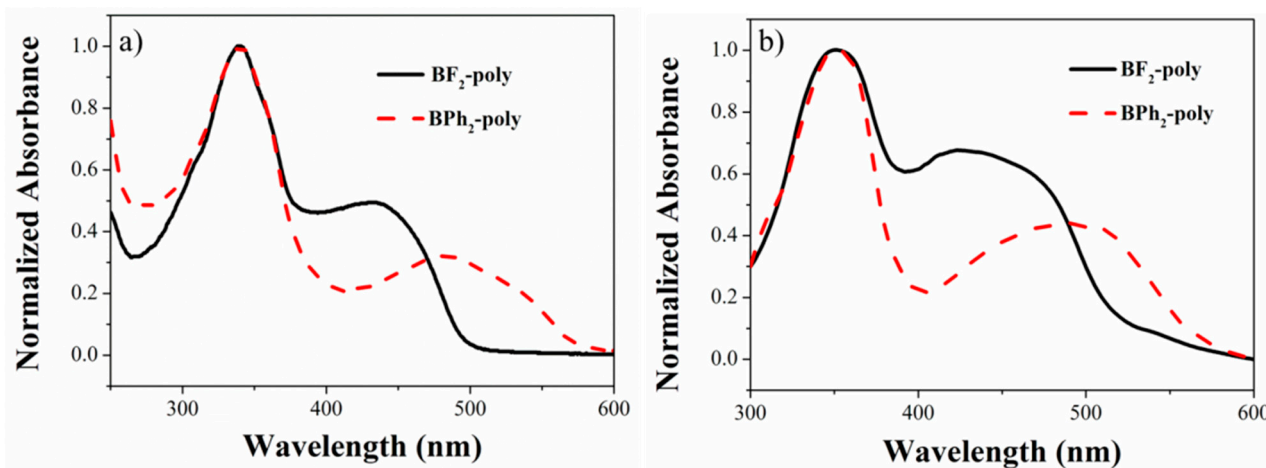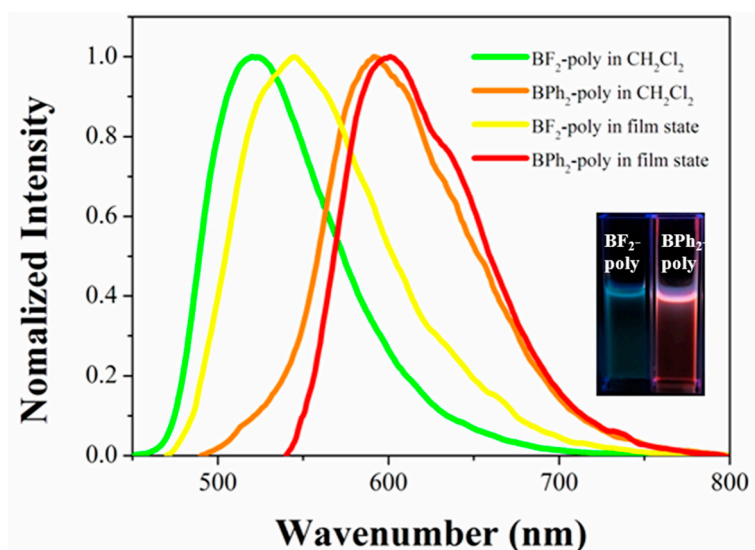

Figure 5. UV–vis spectra of **BF₂-poly** and **BPh₂-poly** in CH_2Cl_2 (**a**) and in solid state (**b**), respectively.

Table 2. Absorption and fluorescence data for relating compounds in CH_2Cl_2 solution.

Samples	λ_{max}	λ_{em}	Stokes Shift	Φ_f
1	410 nm	486 nm	3810 cm^{-1}	0.63
2	468 nm	573 nm	3920 cm^{-1}	0.32
BF₂-poly	433 nm	520 nm	3860 cm^{-1}	0.23
BPh₂-poly	481 nm	592 nm	3900 cm^{-1}	0.11

Films of boron-chelated polymers on quartz plates used for absorption and fluorescence investigations were prepared by spin-coating from a CH_2Cl_2 solution. The absorption maxima of the boron-chelated polymers in thin films shown in Figure 5b were almost identical to those in solution, which indicated that there was nearly no change in conformation of the boron-chelated polymers from the solution to the solid state. In addition, the absorption results of boron-chelated polymers in thin films were used to calculate the band gap values in electrochemical analysis. The fluorescence spectra of the boron-chelated polymers showed significant differences between in CH_2Cl_2 solution and in the solid state (Figure 6). **BF₂-poly** and **BPh₂-poly** showed emission peaks at 545 nm and 601 nm, respectively. The maximum emission peaks of **BF₂-poly** and **BPh₂-poly** exhibited red shift of 25 and 9 nm in the solid state. This can be ascribed to the stronger self-absorption effect and a higher degree of ordering in solid state than those in solution. However, the reason for the difference in red shift values from solution to the solid state between two different boron-chelated polymers is still not clear.

**Figure 6.** Fluorescence spectra of **BF₂-poly** and **BPh₂-poly** in CH_2Cl_2 and the solid state.

3.3. Electrochemical Analyses

The electrochemical behaviors of **BF₂-poly** and **BPh₂-poly** were investigated by cyclic voltammetry (CV) with a standard three-electrode electrochemical cell in anhydrous acetonitrile solution at room temperature with 0.1 M tetrabutylammonium hexafluorophosphate (TBAPF6) as a supporting electrolyte to test their electron affinity. The oxidation potentials were measured *versus* $Ag/AgNO_3$ as the reference electrode and a standard ferrocene/ferrocenium redox system as the internal standard for estimating the HOMO of the boron-chelated polymers films. A glassy carbon electrode was used as a working electrode. A platinum sheet was used as an auxiliary electrode. Figure 7 shows the cyclicvoltammograms of boron-chelated polymers in the solid state at a scan rate of 50 mV·s⁻¹ in the range of −1.7–2.0 V. **BF₂-poly** displayed one oxidation peak at +1.40 V. In comparison, **BPh₂-poly** presented two oxidation peaks at +0.69 V and +1.52 V. The HOMO value was estimated by the oxidation peaks in CV curves. The band gap (ΔE) of boron-chelated polymers was obtained from a calculation of $1240/\lambda$, where λ is the value of adsorption edge obtained from Figure 5b. The HOMO–LUMO gaps of **BF₂-poly** and **BPh₂-poly** based on UV–Vis absorption spectra in solid state were calculated as 2.34 eV and 2.11 eV,

respectively. The LUMO value was calculated according to the following Equation: $E_{LUMO} = E_{HOMO} + E_{gap}$. The results are summarized in Table 3.

Table 3. The highest occupied molecular orbital (HOMO) and lowest unoccupied molecular orbital (LUMO) energies and band gap data of boron-chelated polymers.

Polymers	HOMO (eV)	LUMO (eV)	band Gap (eV)
BF₂-poly	−5.89	−3.55	2.34
BPh₂-poly	−5.31	−3.20	2.11
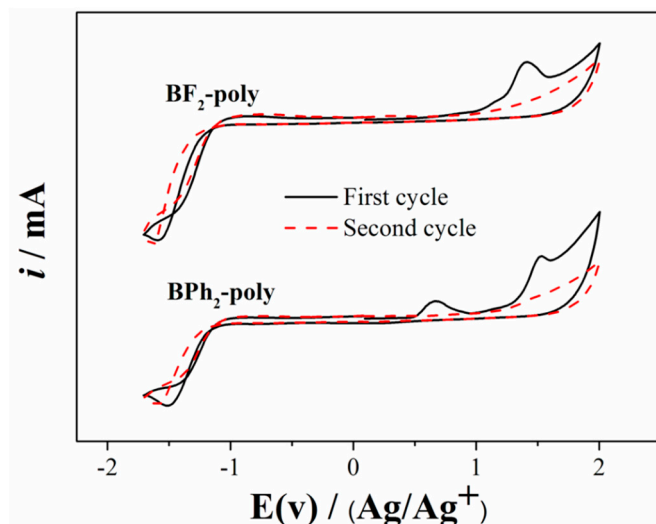
Figure 7. Cyclic voltammograms of **BF₂-poly** (**a**) and **BPh₂-poly** (**b**) in the solid state.

4. Conclusions

In conclusion, we have synthesized organoboron heterochrysene polymers by chelating reaction of 2,2'-pyridoin-based polyfluorene derivative as a polymeric ligand with BF₃·Et₂O or BPh₃. Obtained boron-chelated polymers possess good solubility in common organic solvents, and their number-average molecular weights were 1.13×10^4 Da and 1.24×10^4 Da, respectively, with polydispersity indexes being 1.86 and 2.12. **BF₂-poly** and **BPh₂-poly** displayed green and red emission, both in solutions and in the solid state. The HOMO values calculated from the cyclic voltammetry were −5.89 V and −5.31 V, respectively. The TGA studies showed desirable thermostable properties of the boron-chelated polymers. All the results suggest that the polymers possess great potential applications in electro-optic field.

Supplementary Materials

Supplementary materials can be accessed at: http://www.mdpi.com/2073-4360/7/6/1192/s1.

Acknowledgments

Author Contributions

Xinwu Ba and Yonggang Wu designed the experiments; Hailei Zhang, Shuli Ma and Dongqin Li performed the experiments; Hailei Zhang wrote the paper.

Conflicts of Interest

The authors declare no conflict of interest.

References

1. Dong, H.; Zhu, H.; Meng, Q.; Gong, X.; Hu, W. Organic photoresponse materials and devices. *Chem. Soc. Rev.* **2012**, *41*, 1754–1808.
2. Bendikov, M.; Wudl, F.; Perepichka, D.F. Tetrathiafulvalenes, oligoacenenes, and their buckminsterfullerene derivatives: The brick and mortar of organic electronics. *Chem. Rev.* **2004**, *104*, 4891–4946.
3. Liu, H.; Xu, J.; Li, Y.; Li, Y. Aggregate nanostructures of organic molecular materials. *Acc. Chem. Res.* **2010**, *43*, 1496–1508.
4. Zheng, H.; Li, Y.; Liu, H.; Yin, X.; Li, Y. Construction of heterostructure materials toward functionality. *Chem. Soc. Rev.* **2011**, *40*, 4506–4524.
5. Xia, X.; Chao, D.; Qi, X.; Xiong, Q.; Zhang, Y.; Tu, J.; Zhang, H.; Fan, H.J. Controllable growth of conducting polymers shell for constructing high-quality organic/inorganic core/shell nanostructures and their optical-electrochemical properties. *Nano Lett.* **2013**, *13*, 4562–4568.
6. Suraru, S.L.; Zschieschang, U.; Klauk, H.; Wurthner, F. A core-extended naphthalene diimide as a *p*-channel semiconductor. *Chem. Commun.* **2011**, *47*, 11504–11506.
7. Feng, L.; Zhu, C.; Yuan, H.; Liu, L.; Lv, F.; Wang, S. Conjugated polymer nanoparticles: Preparation, properties, functionalization and biological applications. *Chem. Soc. Rev.* **2013**, *42*, 6620–6633.
8. Williams, E.; Ang, T.; Ooi, Z.; Sonar, P.; Lin, T.; Neo, W.; Song, J.; Hobley, J. Optical characterization of the hole polaron in a series of diketopyrrolopyrrole polymers used for organic photovoltaics. *Polymers* **2015**, *7*, 69–90.
9. Clar, E. *Polycyclic hydrocarbons*; Academic Press: London, UK, 1964.
10. Li, G.; Wu, Y.; Gao, J.; Wang, C.; Li, J.; Zhang, H.; Zhao, Y.; Zhao, Y.; Zhang, Q. Synthesis and physical properties of four hexazapentacene derivatives. *J. Am. Chem. Soc.* **2012**, *134*, 20298–20301.
11. Gu, P.Y.; Zhou, F.; Gao, J.; Li, G.; Wang, C.; Xu, Q.F.; Zhang, Q.; Lu, J.M. Synthesis, characterization, and nonvolatile ternary memory behavior of a larger heteroacene with nine linearly fused rings and two different heteroatoms. *J. Am. Chem. Soc.* **2013**, *135*, 14086–14089.
12. Kivelson, S.; Chapman, O.L. Polyacene and a new class of quasi-one-dimensional conductors. *Phys. Rev. B* **1983**, *28*, 7236–7243.
13. Bendikov, M.; Duong, H.M.; Starkey, K.; Houk, K.N.; Carter, E.A.; Wudl, F. Oligoacenes: Theoretical prediction of open-shell singlet diradical ground states. *J. Am. Chem. Soc.* **2004**, *126*, 7416–7417.

14. Xiao, J.; Duong, H.M.; Liu, Y.; Shi, W.; Ji, L.; Li, G.; Li, S.; Liu, X.W.; Ma, J.; Wudl, F.; *et al.* Synthesis and structure characterization of a stable nonatwistacene. *Angew. Chem. Int. Ed.* **2012**, *51*, 6094–6098.

15. Li, Y.; Xu, L.; Liu, T.; Yu, Y.; Liu, H.; Li, Y.; Zhu, D. Anthraceno–perylene bisimides: The precursor of a new acene. *Org. Lett.* **2011**, *13*, 5692–5695.

16. Kaur, I.; Jazdzyk, M.; Stein, N.N.; Prusevich, P.; Miller, G.P. Design, synthesis, and characterization of a persistent nonacene derivative. *J. Am. Chem. Soc.* **2010**, *132*, 1261–1263.

17. Tonshoff, C.; Bettinger, H.F. Photogeneration of octacene and nonacene. *Angew. Chem. Int. Ed.* **2010**, *49*, 4125–4128.

18. Nepomnyashchii, A.B.; Bard, A.J. Electrochemistry and electrogenerated chemiluminescence of bodipy dyes. *Acc. Chem. Res.* **2012**, *45*, 1844–1853.

19. Lovell, J.F.; Liu, T.W.; Chen, J.; Zheng, G. Activatable photosensitizers for imaging and therapy. *Chem. Rev.* **2010**, *110*, 2839–2857.

20. Chang, C.C.; Hsieh, M.C.; Lin, J.C.; Chang, T.C. Selective photodynamic therapy based on aggregation-induced emission enhancement of fluorescent organic nanoparticles. *Biomaterials* **2012**, *33*, 897–906.

21. Tamgho, I.S.; Hasheminasab, A.; Engle, J.T.; Nemykin, V.N.; Ziegler, C.J. A new highly fluorescent and symmetric pyrrole-BF_2 chromophore: BOPHY. *J. Am. Chem. Soc.* **2014**, *136*, 5623–5626.

22. Ulrich, G.; Ziessel, R.; Harriman, A. The chemistry of fluorescent bodipy dyes: Versatility unsurpassed. *Angew. Chem. Int. Ed.* **2008**, *47*, 1184–1201.

23. Frath, D.; Massue, J.; Ulrich, G.; Ziessel, R. Luminescent materials: Locking π-conjugated and heterocyclic ligands with boron(III). *Angew. Chem. Int. Ed. Engl.* **2014**, *53*, 2290–2310.

24. Nagai, A.; Kokado, K.; Nagata, Y.; Chujo, Y. 1,3-diketone-based organoboron polymers: Emission by extending π-conjugation along a polymeric ligand. *Macromolecules* **2008**, *41*, 8295–8298.

25. Qin, Y.; Kiburu, I.; Shah, S.; Jakle, F. Synthesis and characterization of organoboron quinolate polymers with tunable luminescence properties. *Macromolecules* **2006**, *39*, 9041–9048.

26. Zhang, H.; Hong, X.; Ba, X.; Yu, B.; Wen, X.; Wang, S.; Wang, X.; Liu, L.; Xiao, J. Synthesis, physical properties, and photocurrent behavior of strongly emissive boron-chelate heterochrysene derivatives. *Asian J. Org. Chem.* **2014**, *3*, 1168–1172.

27. Chen, H.; He, M.; Pei, J.; Liu, B. End-group analysis of blue light-emitting polymers using matrix-assisted laser desorption/ionization time-of-flight mass spectrometry. *Anal. Chem.* **2002**, *74*, 6252–6258.

28. Tolman, C.A.; Seidel, W.C.; Gerlach, D.H. Triarylphosphine and ethylene complexes of zerovalent nickel, palladium, and platinum. *J. Am. Chem. Soc.* **1972**, *94*, 2669–2676.

29. Heek, T.; Fasting, C.; Rest, C.; Zhang, X.; Wurthner, F.; Haag, R. Highly fluorescent water-soluble polyglycerol-dendronized perylene bisimide dyes. *Chem. Commun.* **2010**, *46*, 1884–1886.